ANALYSIS OF VORTEX ON SHARP-EDGED DELTA WING WITH BLOWING EFFECT

Muhammad Faris Aqil Zamzuddin[a], Mazuriah Said[b], Nur Amalina Musa[b], Khushairi Amri Kasim[a] and Shabudin Mat[a]*

[a]Faculty of Mechanical Engineering, Universiti Teknologi Malaysia, 81310 UTM Johor Bahru, Johor.
[b]Faculty of Engineering, City University Malaysia, No.8, Menara City U, Jalan 51a/ 223, 46100 Petaling Jaya, Selangor.

Article history
Received
7th December 2022
Received in revised form
22nd June 2023
Accepted
22nd June 2023
Published
30th June 2023

*Corresponding author
shabudin@utm.my

ABSTRACT

The formation of the primary vortex above the wing is dependent on the Reynolds number, the angle of
attack, the Mach number, and the bluntness of the leading edge. This experiment is done to assess the impacts of blowing at three sites on the delta wing's flow topology. The blower was placed on the leading edge at the 15%, 50%, and 70 % wing sections. The experiment was conducted at a Reynolds number of 8 x 105, which corresponds to a wind speed of 25 m/s and a mean aerodynamic chord. The UTM generic delta wing model with a 55° sweep angle was employed, and the experiment was conducted at the Low-Speed Wind Tunnel at Universiti Teknologi Malaysia (UTM-LST). During each experiment, the model was subjected to surface pressure monitoring techniques. This project's findings show the influence of blowing on the flow topology above the wing. In particular test scenarios, placing the blower at the 50 percent mark resulted in a notable enlargement of the main vortex, while also causing a delay in its disintegration at higher angles of attack.

KEYWORDS

Sharp-edged Delta Wing, Vortex Flow Experiment, Active Flow Control, Primary Vortex, Wind Tunnel Testing

1.0 INTRODUCTION

The well-known and typical delta wing flow physics begins with a split at low attack angles at the strongly swept leading edges. The split shear layer forms a large-scale vortex over each half of the wing by rolling upwards. Therefore, fully developed, and stable leading-edge vortices produce increased lift and a rise in maximum angle of attack, which considerably improves the maneuverability of high-agility aircraft [1]

Because primary separation is constant and leading-edge vortex growth is less susceptible to Reynolds number effects, delta wing research frequently employs sharp leading-edge designs [2].

Consequently, the leading-edge radius, angle of attack, and Reynolds number are the primary parameters affecting the commencement of vortex growth as well as the position and strength of the primary vortex, whereas the angle of attack is the primary parameter solely in the event of a sharp leading edge. By self-induction, the separated boundary layer rolls up and forms a secondary vortex, whose spin is opposite to that of the leading-edge (primary) vortex. The generation of secondary vortices is highly dependent upon

the presence of a laminar or turbulent boundary layer [3].

In addition, leading-edge vortices are susceptible to breakdown at high attack angles. Vortex breakdown is generated by the stagnation of the low-energy axial core flow as a result of a rising unfavorable pressure gradient along the vortex axis [4].

2.0 LITERATURE REVIEW

2.1 Flow Separation

According to previous research, the separation of flow at the leading edge is the underlying principle of vortex generation. Flow separation is the separation of the flow from the body. An adverse pressure gradient is one of the factors that generate flow separation. As a result of a larger adverse pressure gradient ($dp/dx > 0$), the flow velocity on the body decreases and finally reaches zero, causing the flow to reverse direction. Separation is more likely to occur in flows with a high Reynold number than in laminar flows.

2.2 Formation of vortex

At a given wind speed and attack angle, the flow on a sharp-edged delta wing may be described as the movement of a portion of the flow from the lower to the upper surface through the leading edge. attached flow is produced on the top side underneath this vortex with an attachment line placed at the center line or at some spanwise location between the center line and the leading edge. The flow near the wing surface is forced outward, and after passing the suction peak under the primary vortex axis, the high adverse pressure gradient at the leading edge generates a second flow separation which is secondary vortex [3]. Vortex flow not only increases the lift but changes the distribution of lift rather drastically [5].

LEV (Leading Edge Vortex) is initially generated by the wing's lower surface. While the flow outboard will go out and attempt to curve around the leading edge to reach the top surface, the flow inboard will travel to spiral around the leading edge to reach the surface as illustrated in Figure 1 [6].

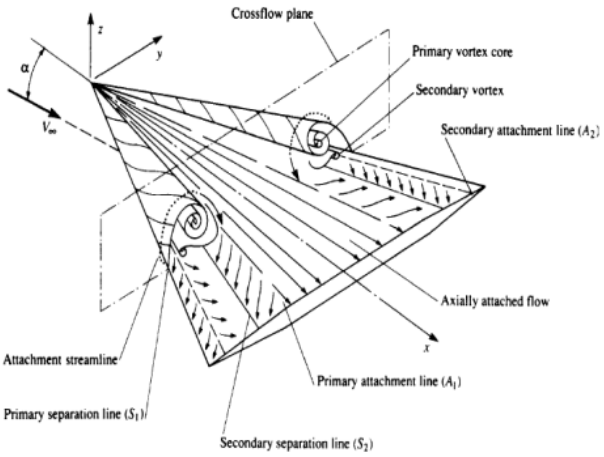

Figure 1: Subsonic Flow on Delta Wing [6]

Mat & Huri [7] state that the pressure distributions were characterized by a Cp trend with minimal variation between them. Consequently, based on the results of his experiment in Figure 2 shows that a change in Reynolds number would not significantly affect the pressure distribution on the delta wing's surface.

An experiment setup with 3 different Reynolds number 80 000, 150 000 and 268 783 by Kwak & Nelson [6], show that the maximum CL value climbs from 1.16 to 1.17 to 1.18 as the Reynolds number increases as shown in Figure 3. This show assertion that Reynolds number has no appreciable effect on delta wing lift.

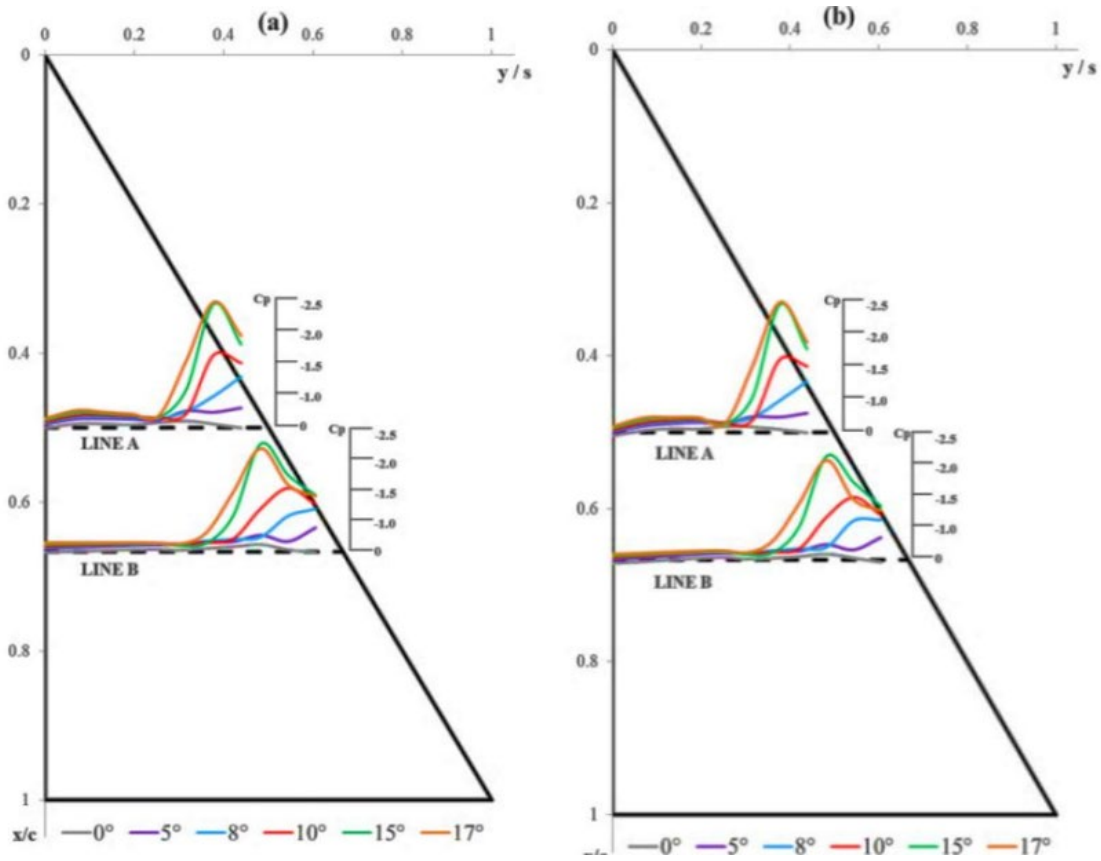

Figure 2: Half-span pressure distribution for 13.5 m/s and 15 m/s [7]

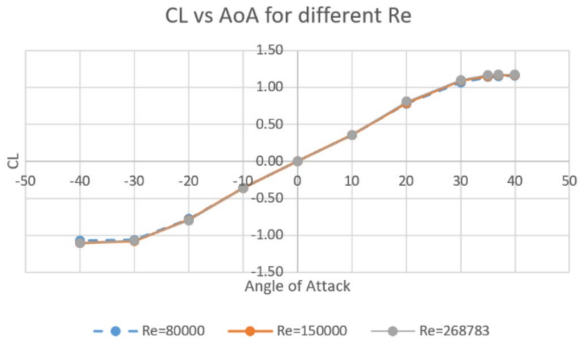

Figure 3: C_L against α [6]

2.3 Vortex breakdown

Furman & Breitsamter [1] said that if an increase in angle of attack does not result in an increase in the primary vortex suction peak, then the leading-edge vortex may break down.

Mat *et al.* [11] also add that at a high angle of attack, vortices undergo a sudden expansion that causes vortex breakdown. This process of vortex disintegration causes unsteadiness in the flow and a significant decrease in lift. Vortex breakdown occurs close to the trailing edge of the wing, causing flow disruptions. Figure 4 shows the experimental vortex breakdown on sharp-edged at α=22.5° done by Mat *et al.* [11].

As the angle of attack grows, the negative pressure gradient in the axial direction of the vortex core also increases, contributing to the breakdown state. If the angle of attack is raised, the breakdown that happens in the trailing edge (relatively high incidence) travels upstream [9].

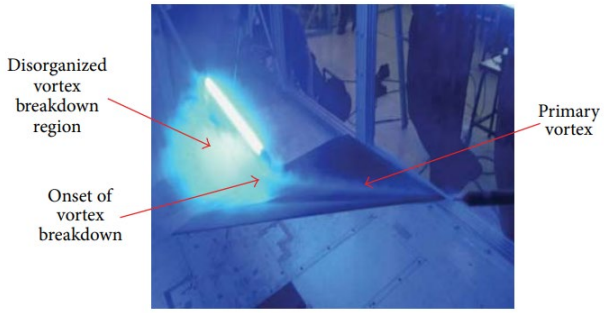

Figure 4: Vortex Breakdown on Sharp-Edged Wing at α = 22.5°

The findings by Polhamus [10], demonstrate that the Reynolds number has little effect on the position of the breakdown. Said [9] state that the flow characteristics of the vortex breakdown very much depend upon the Reynolds number, angle of attack, and leading-edge bluntness and suggest investigation needs more experiments in the future.

2.4 Flow control

The flow control approach can be classified as active and passive ways. Active flow control involves the expenditure of energy to regulate the flow. Control surface techniques such as leading-edge flaps and variable leading-edge extension, pneumatic devices such as blowing/suction, and plasma actuators are examples of active flow control techniques. Methods for passive flow control include the creation of numerous vortex systems and the modification of leading-edge morphologies. Either a double delta wing or canards/strakes/forebodies can be used to generate multiple vortices. With the decrease in sweep angle, it appears challenging to delay vortex collapse. Even at low incidences, vortex breakdown occurs on non-slender wing surfaces. This may be because low-swept wings experience a higher unfavorable pressure gradient than high-swept wings [8].

3.0 RESEARCH METHODOLOGY

For this undertaking, a delta-wing unmanned aerial vehicle (UAV) concept was selected, featuring a pointed front edge and a sweep angle of 55 degrees. This design deviates from being slender, as depicted in Figure 5. The delta wing's specifications are provided in Table 1. The wing was manufactured using aluminum and incorporated 102 pressure taps located on the upper surface. These pressure taps were positioned at specific locations: 10%, 20%, 40%, 65%, 75%, and 90% of the wing's chord length (y/cr) from the apex. Additionally, as part of the study, six holes were drilled into the leading edge of the wing.

The purpose of constructing this model with a sharp leading edge is to examine the impacts of angle of attack with different blower configurations and flow topologies above the wing. At Reynolds number $0.8x10^6$ and equal wind speeds of 25 m/s, tests were conducted with attack angles ranging from 0° to 18° degrees. Mean Aerodynamic Chord (MAC) of 0.4937m is used to compute Reynolds number.

Only three holes are required for the analysis, while the remaining three are for model stability during testing. The blowing rate was given by the compressor and supplied to the model via tubes that were installed. The holes are positioned at three specific locations relative to the core's apex. The first location, denoted as I, is situated 15 percent away from the apex or approximately 148.5 mm. The second location, referred to as II, is positioned 30 percent away from the apex or around 297 mm. Finally, the third location, also designated as II, is located 70 percent away from the apex or approximately 297 mm.

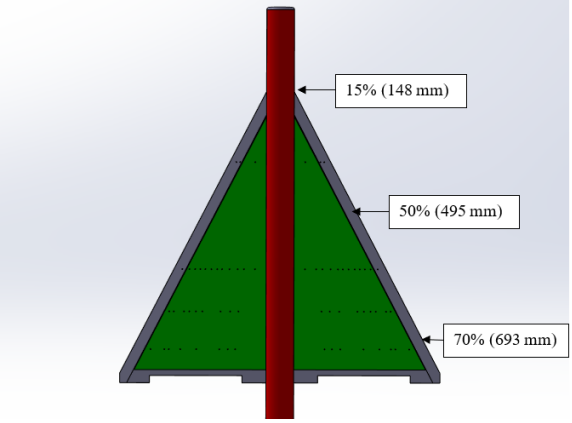

Figure 5: Delta Wing Model

Table 1: Delta Wing Specification

Parameter	Dimension
Length of fuselage	990 mm
Sweep angle	55°
Maximum wingspan	1062 mm
Maximum wing chord	742 mm
Mean aerodynamic chord	493.7 mm
Fuselage diameter	65 mm
Height	215 mm

The experiment took place in the Low-Speed Wind Tunnel (UTM-LST) at Universiti Teknologi Malaysia, which has dimensions of 2.0m in width, 1.5m in height, and 5.8m in length. The wind tunnel can reach a maximum speed of 80 m/s. The experiments were conducted at a velocity of 25 m/s, corresponding to Reynolds numbers of 8 x 10^5. Various angles of attack were tested, ranging from 0° to 18° with a 3° increment. Figure 6 illustrates the experimental setup in the test section.

Figure 6: Experiment Setup in UTM-LST

The pressure distribution on the delta wing's surface was measured using pressure tubes inserted into the wing, assisted by a pressure scanner as shown in Figure 7. The data was recorded using the LabView application within the wind tunnel facility. To inflate the model's surface, a compressor was employed. Six pairs of tubes were installed, running from the compressor to the speed regulator, which controlled the airflow. The wind speed for this experiment was set at 35 m/s. From the speed regulator, the airflow passed through manifolds.

Figure 7: Pressure Scanner

4.0 RESULTS

This section discusses the experiment's surface pressure measurement result. The raw data was processed to evaluate the flow under two major conditions which is (a) clean configuration and (b) blowing effect at location 1, 2, 3 which correspond to configuration 1,2 and 3. For Clean configuration, it will be tested to confirm that increasing angle of attack have been one of the factors that impact the development of primary vortex. Blowing configuration will be compared to the clean to see whether the blower have impact on delta wing.

4.1 Clean configuration

Figures below illustrate the results obtained for a Reynolds number of 0.8 x 10^5. Figure 8, 9 and 10 depict the coefficient of pressure on the wing surface at α = 6°, 12°, and 18°. The three angles were chosen to represent the low, medium, and high attack angles, respectively. The main vortex forms at about 40% of the apex for both α = 6° and α = 12° in Figure 8 and Figure 9, while the primary vortex forms at around 20% for α = 18° in Figure 10.

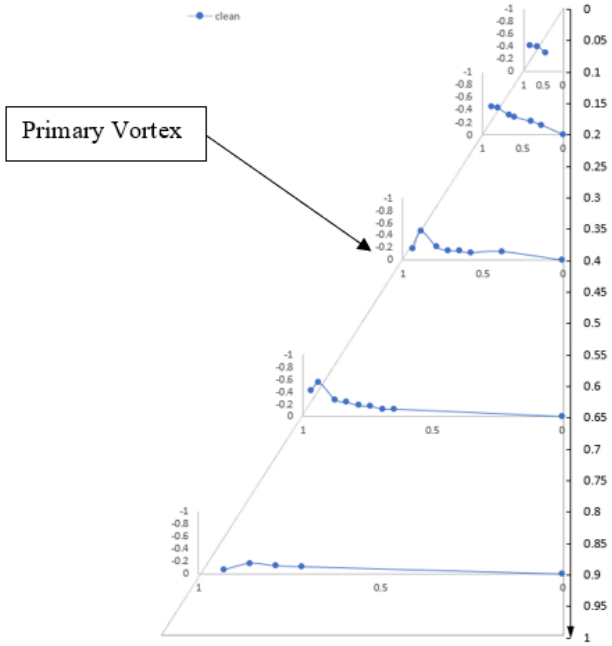

Figure 8: Clean Configuration at α = 6°

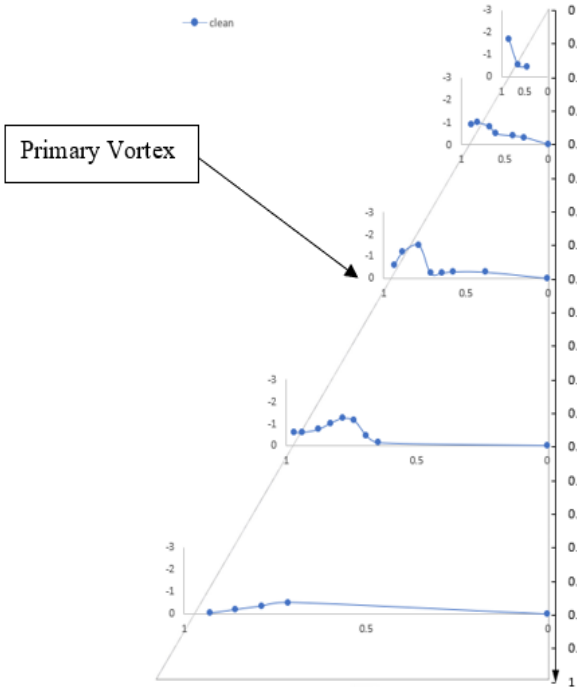

Figure 9: Clean Configuration at α = 12°

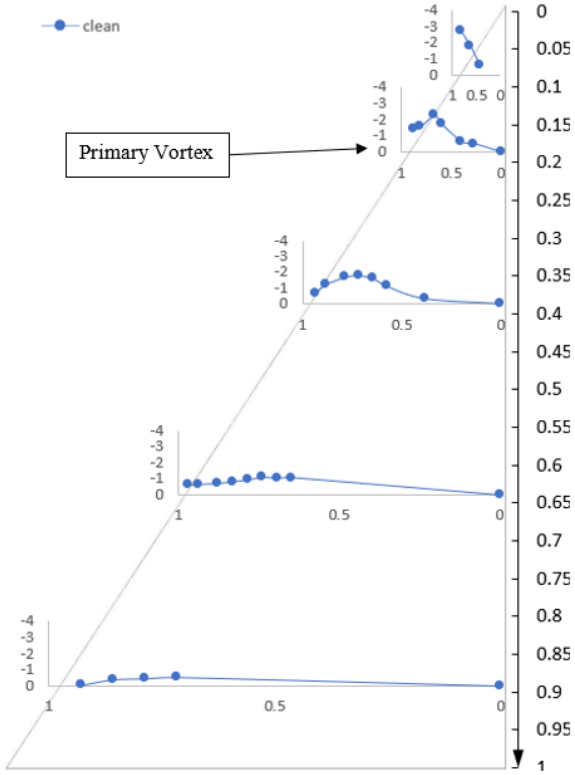

Figure 10: Clean Configuration at α = 18°

4.2 Blower Configuration Low Angle of Attack

The selected angles for the low angle of attack area are 3° and 6°. Figure 11 illustrates the combination graph of all blowing location points at α = 3°. According to the graph, there are no improvements in C_P. This was result of low flight speeds which a delta-wing aircraft must fly at a high angle of attack to obtain the required lift coefficient [12].

As the blowing at position II and III for the α = 6° in Figure 12, there is no significant changes compared to the clean configuration. Mat *et al*. [8] clarified that the flow is attached at low angle of attack with the absence of the leading-edge vortex. Thus, blowing has less impact on the normal force coefficient for low angle of attack.

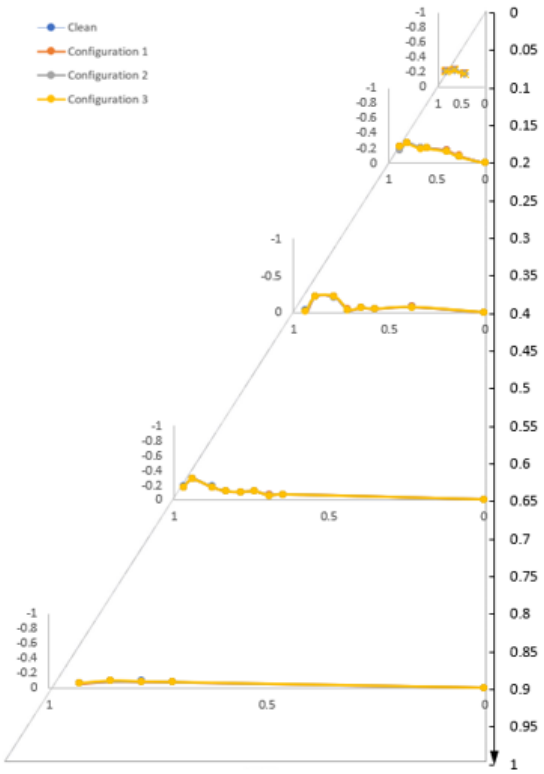

Figure 11: C_P graph for all configuration at α = 3°

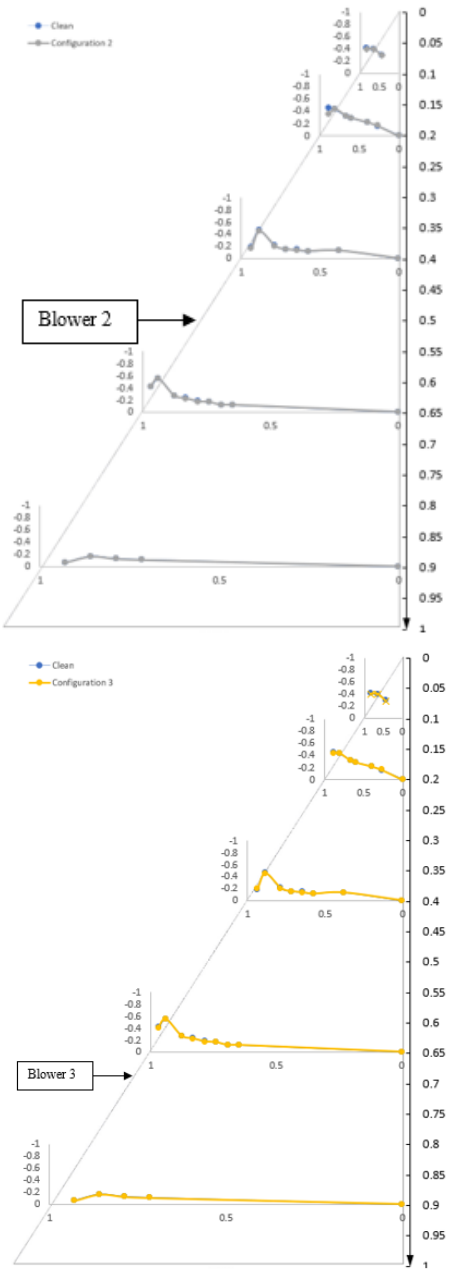

Figure 12: Cp graph for configuration 2 and 3 at α = 6°

4.3 Blower Configuration Medium Angle of Attack

The designated angles for the medium angle of attack range are 9° and 12°, as depicted in Figure 13. At these angles, the flow remains attached to the leading edge but starts to separate and shift towards the area where the core of the vortex is situated. At 9°, the primary vortex appears at 65% of the apex, whereas at α = 12°, the main vortex emerges at 40% of the apex. When it comes to the medium angle of attack, the effects of blowing at positions I and III are not evident from all angles, except for position II.

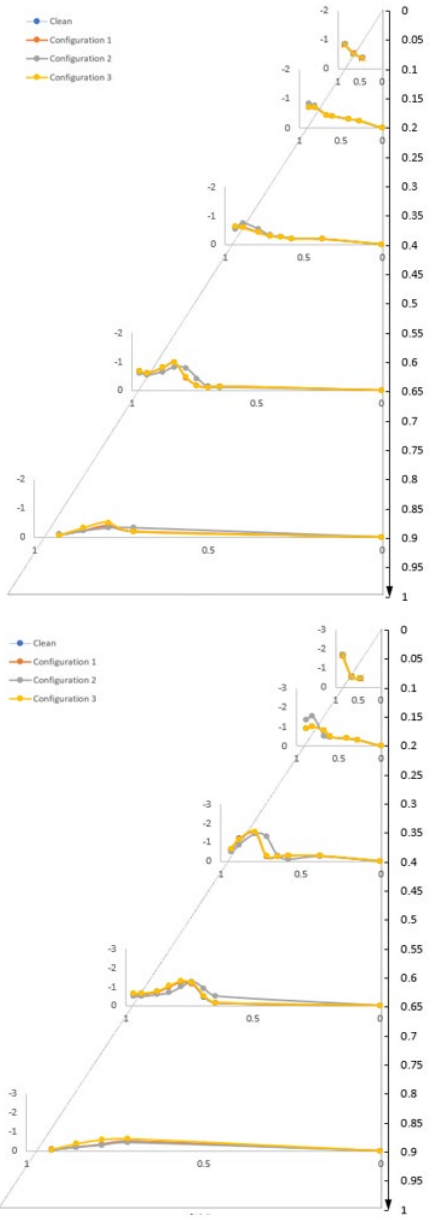

Figure 13: Cp graph for all configuration at α = 9° and α = 12°

For configuration 2 which blowing at position 2, we can see that blowing have significant effects towards development of primary vortex. The primary vortex appears at y/cr = 0.65 and y/cr = 0.4 for 9° and 12° respectively. From Figure 14, we can see improvement which the main vortex shifted to the center of delta wing for α = 9° at y/cr =0.65 and y/cr =

0.9 while for α =12° the shift occurs at y/cr = 0.4 and y/cr = 0.65.

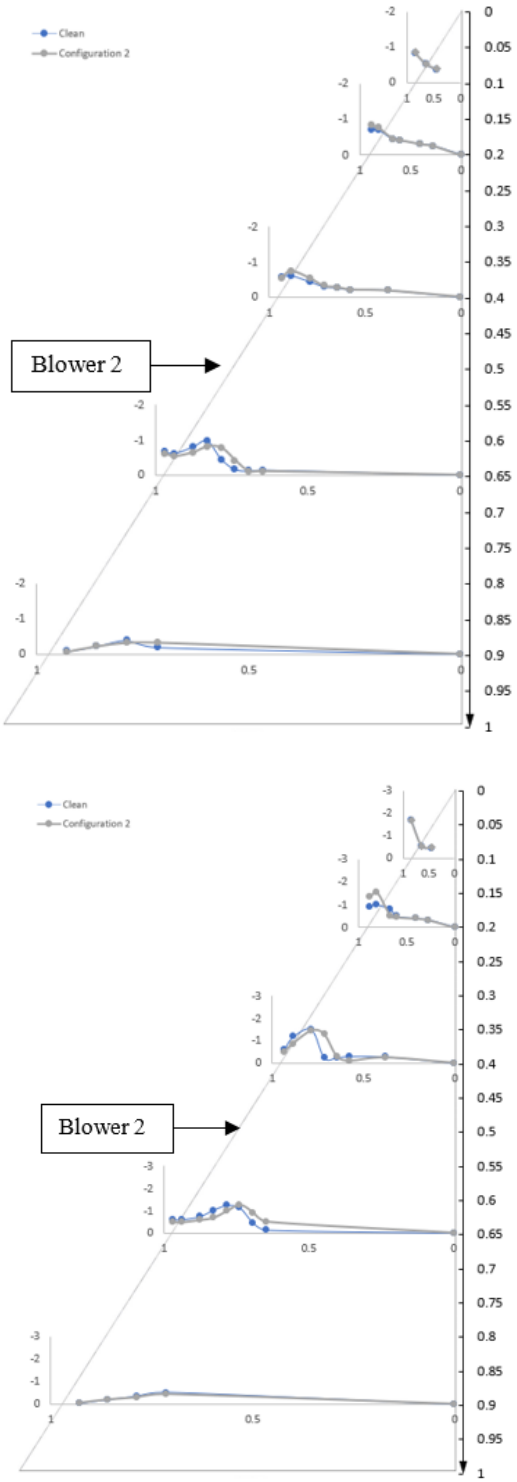

Figure 14: Cp graph for configuration 2 at α = 9° and α = 12°

4.4 Blower Configuration High Angle of Attack

Between the attack angles of 15° and 18°, there is a noticeable enlargement of the primary vortex at the leading edge, as depicted in Figure 15. The flow has become detached from the wing, leading to a significant increase in the suction peak. The impact of blowing at attack angles of 15° and 18° for configuration II is evident in Figure 16. Blowing at position II results in an increase in the pressure coefficient at y/cr = 20%, 40%, and 65% for both 15° attack angle scenarios. Positions I and III, on the other hand, indicate that the pressure coefficient remains unchanged at high angles of attack.

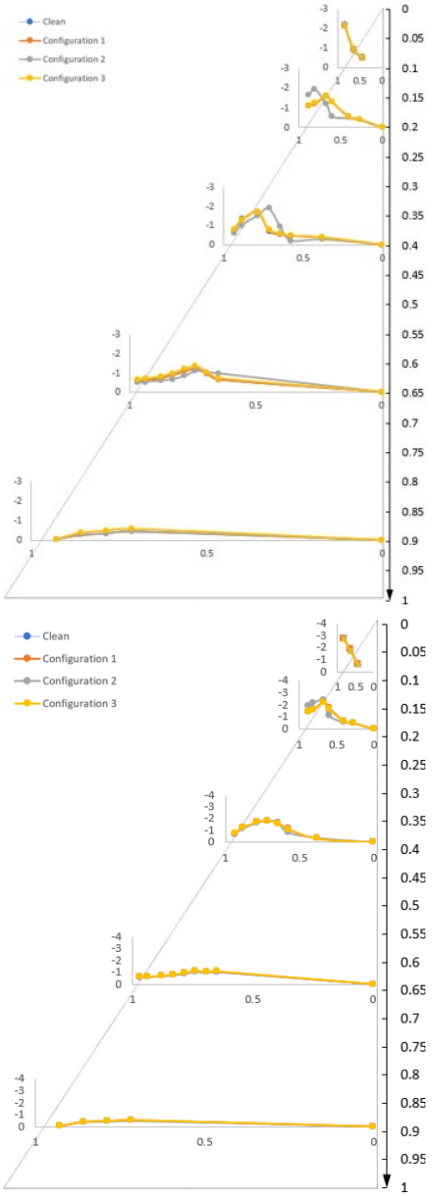

Figure 15: Cp graph for all configuration at α = 15° and α = 18°

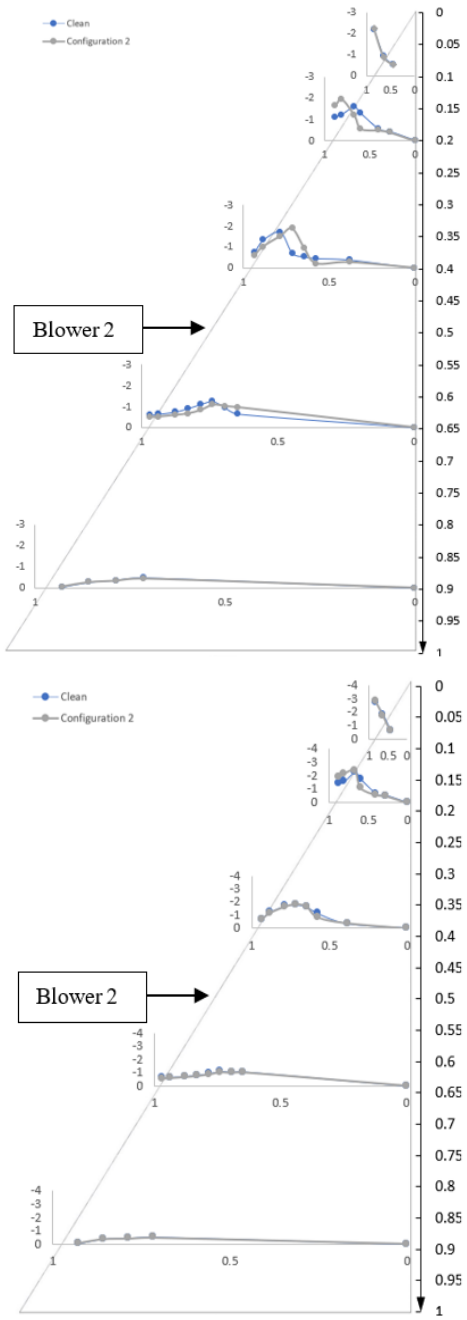

Figure 16: Cp graph for configuration 2 at α = 15° and α = 18°

5.0 CONCLUSION

The airflow over a non-slender delta wing with a sharp edge exhibits a complex vortex structure. The aim of this project was to investigate how different blowing locations affect the vortex characteristics of a sharp-edged, non-slender delta wing model. The surface pressure measurement approach was utilized in a wind tunnel experiment. The surface pressure coefficient graph shows that the blowing has influenced the flow on the surface of the delta wing. The development and breakdown of the primary vortex was impacted by the blower location. As the conclusion, the blowing at position 1 for lower angle of attack were not significant as the flow still intact on the surface meanwhile at medium and higher angle of attack, blowing at position 1 and 3 has minor improvement. Blowing at position 2 has noticeable impact on magnitude of primary vortex thus delaying the vortex breakdown.

6.0 RECOMMENDATION

Testing with increased diameter of hole, increasing the blowers' mass flow rate, and changing the position of blower may give better results. On the other hand, the experiment was limited to only 6 positions of pressure tap along the chordwise position. Increasing the number of locations might give more detail on vortex development and breakdown.

REFERENCES

1. A. Furman and C. Breitsamter, "Turbulent and unsteady flow characteristics of delta wing vortex systems," *Aerosp. Sci. Technol.*, vol. 24, no. 1, pp. 32–44, 2013, doi: 10.1016/j.ast.2012.08.007.
2. J. M. Luckring, "Reynolds number and leading-edge bluntness effects on a 65° delta wing at transonic speeds," *41st Aerosp. Sci. Meet. Exhib.*, no. January, 2003.
3. D. Hummel, "Effects of Boundary Layer Formation on the Vortical Flow above Slender Delta Wings," *RTO AVT Spec. Meet. "Enhancement NATO Mil. Flight Veh. Perform. by Manag. Interact. Bound. Layer Transit. Sep.*, no. October, pp. 4–7, 2004.
4. A. Mitchell *et al.*, "OF VORTEX BREAKDOWN FLOW FIELD AND SURFACE MEASUREMENTS 38th Aerospace Sciences Meeting & Exhibit," no. c, 2000.
5. E. C. Polhamus, "Sharp-Edge Delta Wings Based O N a Leading-Edge-Suction Analogy," *Natl. Aeronaut. Sp. Adm.*, pp. 1–16, 1966.
6. I. B. Hamizi and S. A. Khan, "Aerodynamics investigation of delta wing at low reynold's number," *CFD Lett.*, vol. 11, no. 2, pp. 32–41, 2019.
7. M. Z. A. D. Huri and S. Mat, "Experimental

Investigation of Delta Wing Flow Behaviour under Pitching Motion," *J. Transp. Syst. Eng.*, vol. 3, pp. 19–24, 2015.

8. S. Gupta, S. Kumar, and R. Kumar, "Control of leading-edge vortices over delta wing using flow control methods: A review," *Mater. Today Proc.*, vol. 50, pp. 2189–2193, 2021, doi: 10.1016/j.matpr.2021.09.447.
9. M. Said, "EFFECTS OF LEADING EDGE RADIUS, REYNOLDS NUMBER AND ANGLE OF ATTACK ON THE VORTEX FORMATION ABOVE LARGE-EDGED DELTA WING," 2016.
10. G. S. West and C. J. Apelt, "BLOCKAGE AND ASPECT RATIO EFFECTS ON FLOW PAST A CIRCULAR CYLINDER FOR 104 less than R less than 105.," *Res. Rep. Ser. - Univ. Queensland, Dep. Civ. Eng.*, vol. 114, no. 29, 1981.
11. S. Mat *et al.*, "Development of Delta Wing Aerodynamics Research in Universiti Teknologi Malaysia Low Speed Wind Tunnel," *Adv. Mech. Eng.*, vol. 2014, 2014, doi: 10.1155/2014/434892.
12. D. Y. Kwak and R. C. Nelson, "Vortical flow control over delta wings with different sweep back angles using DBD plasma actuators," *5th Flow Control Conf.*, no. July, pp. 1–10, 2010, doi: 10.2514/6.2010-483